

Showcasing research from Heterogenous Catalysis's Laboratory/KAUST Catalysis Center (KCC), King Abdullah University of Science and Technology (KAUST), Thuwal, Saudi Arabia

Well-defined silica-supported zirconium-imido complexes mediated heterogeneous imine metathesis

Well-defined silica-supported zirconium-imido complexes effectively catalyze imine/imine cross-metathesis and are thus considered as the first heterogeneous catalysts active for imine metathesis.

As featured in:



See Jean-Marie Basset et al.,
Chem. Commun., 2016, **52**, 4617.



Cite this: *Chem. Commun.*, 2016, 52, 4617

Received 18th January 2016,
Accepted 14th February 2016

DOI: 10.1039/c6cc00471g

www.rsc.org/chemcomm

Upon prolonged thermal exposure under vacuum, a well-defined single-site surface species $[(\equiv\text{Si}-\text{O}-)\text{Zr}(\text{NEt}_2)_3]$ (1) evolves into an ethylimido complex $[(\equiv\text{Si}-\text{O}-)\text{Zr}(\equiv\text{N}\text{Et})\text{NEt}_2]$ (2). Reactions of 2 with an imine substrate in imido/imine ($\equiv\text{NR}$, R: Et, Ph) exchange (metathesis) with the formation of $[(\equiv\text{Si}-\text{O}-)\text{Zr}(\equiv\text{NPh})\text{NEt}_2]$ (3). Compounds 2 and 3 effectively catalyze imine/imine cross-metathesis and are thus considered as the first heterogeneous catalysts active for imine metathesis.

Surface organometallic chemistry (SOMC) has allowed the access to a rich library of surface complexes active for a wide range of catalytic reactions. The nature of the fragments ($\text{M}=\text{C}$, $\text{M}-\text{C}$, $\text{M}-\text{H}$, $\text{M}-\text{NC}$) borne by the supported metal is pivotal to its reactivity toward targeted catalysis (*e.g.* alkane metathesis,¹ alkene metathesis,² methane nonoxidative coupling). Surface $[\text{M}]=\text{NR}$ fragments have not been well-investigated within this framework and their characterization and reactivity studies remain limited to date.

In the general context of both homogeneous and heterogeneous catalyses, transition metals forming multiple bonds with ligands are key in several industrially important chemical processes such as alkane oxidation^{3–5} ($\text{M}=\text{O}$) or alkene metathesis^{6–8} ($\text{M}=\text{CR}_2$). In contrast, their metal imide ($\text{M}=\text{NR}$) counterparts have received less attention yet can act as an intermediate in imido group ($\equiv\text{NR}$) transfer reactions.⁹ The importance of imido complexes and their isolable analogues is well-established in organic synthesis and catalysis.^{10,11} Stoichiometric or catalytic reactions may occur at the $\text{M}=\text{NR}$ fragment itself,¹² or the imido group may remain a spectator, as in Schrock's group 6 olefin metathesis catalysts¹³ and imido-based Ziegler–Natta type olefin polymerisation catalysts.¹⁴ Catalytic imine metathesis is analogous to olefin metathesis in that two different

imines afford a statistical mixture of all possible $\equiv\text{NR}$ exchange products.



Imine/imide exchange reactions for which mechanistic data were reported apparently may proceed by two separate pathways. On the one hand, Bergman and co-workers established a Chauvin type mechanism based on isolable diazametallacyclic intermediates in the reaction of $\text{CpCp'}\text{Zr}(\equiv\text{NR})(\text{THF})$ ($\text{Cp}' = \text{Cp}, \text{Cp}^*$) with imines.^{15–17} On the other hand, kinetic studies by Mountford and co-workers support an amine-catalyzed process to explain the reaction of $(\text{py})_3\text{Cl}_2\text{Ti}(\equiv\text{NR})$ with imines.^{9,18}

More recently, imine metathesis (eqn (1)) catalyzed by transition metals (Zr ,^{15–17} Ti ,⁹ Mo ,¹⁹ Re ,²⁰ Ta ,²¹ Nb^4) was investigated in a number of research groups, most likely on account of the mechanistic analogy with the more famous and synthetically relevant olefin metathesis.^{22,23} To date, heterogeneous catalysts for imine metathesis have not been reported. Our recent foray into silica supported zirconium amido catalysts^{24,25} encouraged us to examine the formation and the reactivity of the related metal imido complexes. Note that $\text{M}=\text{N}$ fragments supported on silica have been documented only as spectator ligands for olefin metathesis molybdenum catalysts.^{26–30}

Herein, we describe both the first catalytic imine metathesis reactions using silica supported imide–zirconium complexes. All surface species were characterized by solid state (SS) NMR experiments, elemental analysis and FT-IR spectroscopy.

The surface complex 1 was prepared by treating SiO_{2-700} with a solution of $\text{Zr}(\text{NEt}_2)_4$ in pentane (1.1 equivalents with respect to surface silanols). After workup, 1 was obtained as a yellow powder containing 2.7% Zr, 4.3% C and 1.3% N with a Zr/C/N molar ratio of 1/12/3.1 (± 0.3) (expected 1/12/3) and thus suggests a monopodal surface complex with three NEt_2 ligands. Comparison of the FT-IR spectra of SiO_{2-700} and 1 (Fig. 1) is consistent with the chemical grafting of $\text{Zr}(\text{NEt}_2)_4$ onto the silica surface.

King Abdullah University of Science and Technology (KAUST), KAUST Catalysis Center (KCC), Thuwal, 23955-6900, Saudi Arabia.

E-mail: jeanmarie.basset@kaust.edu.sa

† Electronic supplementary information (ESI) available: Detailed experimental procedures, additional data, and figures and tables. See DOI: 10.1039/c6cc00471g



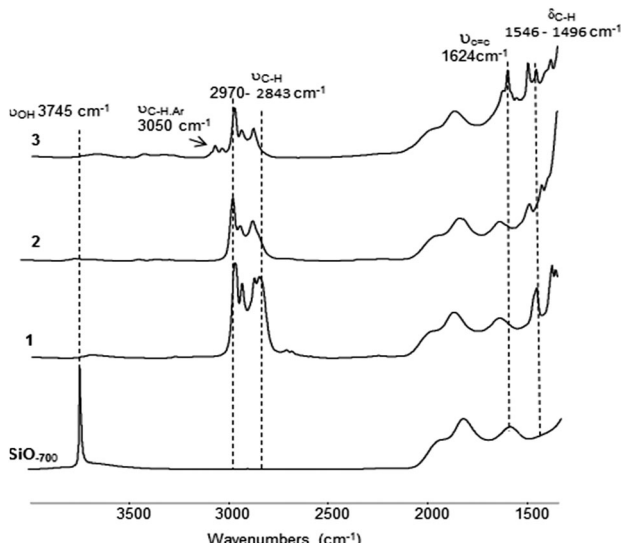


Fig. 1 FT-IR of SiO_2 -700, **1** [$\equiv \text{Si}-\text{O}-\text{Zr}(\text{NEt}_2)_3$], **2** [$\equiv \text{Si}-\text{O}-\text{Zr}(\equiv \text{NEt})\text{NEt}_2$] and **3** [$\equiv \text{Si}-\text{O}-\text{Zr}(\equiv \text{NPh})\text{NEt}_2$].

The IR peaks associated with the isolated surface silanols (3745 cm^{-1}) completely disappeared. Conversely, new IR bands associated with $\nu(\text{CH})$ and $\delta(\text{CH})$ of the diethylamine ligands are observed in the $2970\text{--}2843 \text{ cm}^{-1}$ and $1546\text{--}1496 \text{ cm}^{-1}$ regions, respectively.

All these observations and chemical analyses are consistent with the proposed structure of **1** (Fig. 2), but further corroborations at the molecular level have been sought using SS NMR spectroscopy of the grafted species. The solid-state ^1H NMR spectrum of **1** shows two broad resonances at 1.1 and 3.2 ppm (Fig. 2A) and its ^{13}C solid-state cross polarization/magic angle spinning (CP/MAS) NMR spectrum displays strong signals at 14 and 43 ppm (Fig. 2B).²⁵

Moreover, the 2D HETCOR SS NMR spectra revealed the correlations between only pairs of attached ^1H - ^{13}C spins using

a short contact time of 0.5 ms. Clear correlations were noticeable between the protons at 1.1 and 3.2 ppm and the carbons at 14 and 43 ppm, respectively (Fig. 2E). Two-dimensional proton double- (DQ) and triple-quantum (TQ) correlation experiments were applied to determine the number of protons attached to the same carbon, hence discriminating between CH_2 and CH_3 groups. A strong autocorrelation peak is observed for the proton resonances at 1.1 ppm in both DQ and TQ spectra (Fig. 2C and D). This is compatible with the assignment of this resonance to methyl protons. The resonances at 3.2 ppm show a correlation at 6.4 ppm (ω_1) in the DQ spectrum, but no autocorrelation peak is observed in the TQ spectrum. It can be thus assigned to a CH_2 group. Furthermore, a correlation in the DQ NMR spectrum between the CH_3 group at 1.1 ppm and the CH_2 group at 3.2 ppm confirms that both groups are in proximity to each other. In conclusion, these data validate **1** as a surface zirconium complex exhibiting three equivalent diethyl-amido ligands [$\equiv \text{Si}-\text{O}-\text{Zr}(\text{NEt}_2)_3$].

The formation of imido ligands during the synthesis of molecular dialkylamido metal complexes is known to occur after thermal treatment under vacuum.³¹ The release of gaseous alkenes and dialkylamines has also been detected upon thermal transformation of isolable dialkylamido³² and imine complexes of the early transition metals.³³ We decided to monitor the thermal treatment of **1** to observe possibly the conversion to zirconium imido surface species (Scheme 1).

The initial evacuation of **1** at room temperature left the IR spectrum unchanged, although evacuation at elevated temperature (200 °C) resulted in the modification of the signal pattern (Fig. 1) concurrently to an overall reduction of the signal's intensity in the alkyl vibration region. Elemental analysis of **2** gives 2.7% Zr, 2.3% C and 0.9% N with a Zr/C/N ratio of 1/6.4/2.1 (± 0.3) (expected 1/6/2). The volatiles identified and quantified by GC consist exclusively of diethylamine and ethylene (1/0.9). The ^1H SS NMR spectrum of **2** contains two broad signals centered at 1.1 and 3.1 ppm (Fig. S1, ESI†). The ^{13}C SS NMR spectrum of **2** (Fig. S2, ESI†) exhibits two major signals at 14.2 and 40.6 ppm and two minor signals at 18.7 and 36.2 ppm. The most intense peaks at 14.2 and 40.2 ppm are reminiscent of that previously seen for **1** at 14 ppm and 42.7 ppm. They were assigned to the carbon atoms of amino-ethyl groups in the $\text{N}(\text{CH}_2\text{CH}_3)_2$ ligands. The other two peaks at 18.7 and 36.2 ppm were consistent with an N -ethyl group different to that already present on the zirconium center. Considering all the data, we can attribute them to the methyl and the methylene group borne by the nitrogen of an ethylimido ligand ($\equiv \text{NCH}_2\text{CH}_3$).

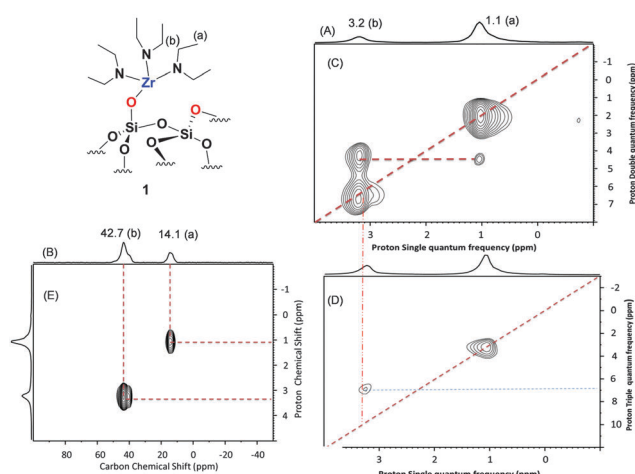
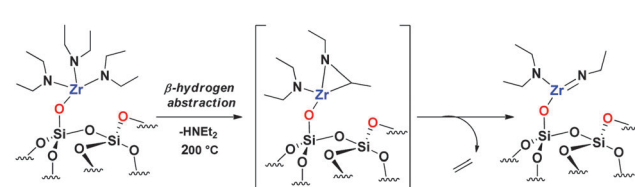
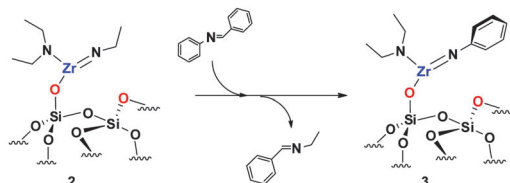


Fig. 2 (A) 1D ^1H spin-echo MAS solid state NMR spectrum of **2**, (B) ^{13}C CP/MAS NMR spectrum of **2**, (C) 2D ^1H - ^1H double-quantum (DQ)/single-quantum (SQ), (D) ^1H - ^1H triple-quantum (TQ)/SQ and (E).



Scheme 1 Silica-supported zirconium imido formation with the hypothetical intermediate.³⁴

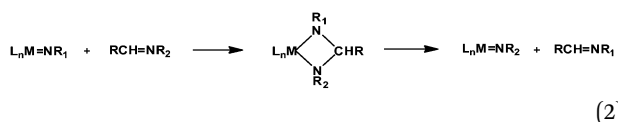




Scheme 2 Silica-supported imide/imine metathesis.

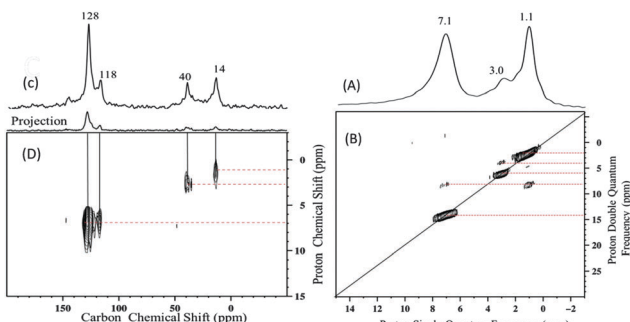
All these results allow us to identify **2** as $[(\equiv \text{Si}-\text{O}-)\text{Zr}(\equiv \text{N}-\text{Et}_2)\text{NEt}_2]$. To the knowledge of the authors, this is the first report of a well-defined single site zirconium imido species supported onto silica.

Previous reports mainly described two types of NR transfer reactions: stoichiometric and catalytic. The former passes by imide/imine stoichiometric metathesis of a metal imide with one molecule of the imine substrate and is regiospecific. New metal imide and imine products are formed by a transient 4-membered metallacycle (eqn (2)).



Treatment of **2** by benzal(benzyl)amine (1.2 eq.) in toluene at 80 °C yielded **3** (Scheme 2). Following filtration, washing and evacuation under high vacuum, **3** showed bands characteristic of the presence of an aromatic group at around 3050 cm⁻¹ (aromatic C-H bending) and one at 1624 cm⁻¹ ($\nu_{\text{C}=\text{C}}$) (Fig. 1). A comparison of the FT-IR spectra of **2** and **3** reveals a notable decrease of ν_{CH} (2970–2843 cm⁻¹). Elemental analysis of **3** gives 2.7% Zr, 3.7% C and 0.95% N with a Zr/C/N ratio of 1/10.3/2.2 (± 0.3) (expected 1/10/2). This is in agreement with one NEt_2 ligand in **2** being replaced by an arylimido ligand.

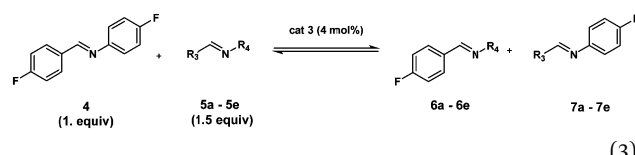
The ¹H NMR spectrum of **3** contains an intense signal at 7.1 ppm (Fig. 3A), absent for **1** and **2**, in addition to two overlapping peaks (a major one at 1.1 ppm and a minor one at 3 ppm). The ¹³C MAS spectrum displays also two new signals at 118 and 128 ppm consistent with aromatic carbon in addition to two signals at 14 ppm and 40 ppm (Fig. 3C). A correlation was observed in the HETCOR spectrum between the ¹H signal at 7.1 ppm and ¹³C signals at 118 and 128 ppm (Fig. 3D).

Fig. 3 (A) 1D ¹H spin-echo MAS solid state NMR spectrum of **3**, (B) 2D ¹H-¹H double-quantum (DQ), (C) ¹³C CP/MAS NMR spectrum of **3**, (D) 2D CP/MAS HETCOR NMR spectrum of **3** (see the ESI† for details).

Moreover, the DQ experiment shows a double autocorrelation for the 7.1 ppm resonance as expected for an aromatic CH proton (Fig. 3B). These observations are in line with the presence of an aromatic group in **3**. In the double-quantum (DQ) spectrum (Fig. 3B), the ¹H signals at 1.1 and 3.0 ppm display strong auto-correlations that can be assigned to the NEt_2 group similarly to that observed in **1**.

Species **3** was investigated as a catalyst for the imine metathesis reaction. Selected imine substrates were tested. All runs were carried out under similar conditions (80 °C, 4 mol% catalyst, toluene (0.4 ml)) and terminated after 2, 4 and 12 h (Table S1, ESI†). The products monitored by gas chromatography-mass spectrometry were consistent with those obtained in cross metathesis reaction (eqn (3)).

Reactions using imines such as *N*-(3,4-methylenedioxybenzylidene)benzylamine (entry 1) and benzal(benzhydryl)amine (entry 2) occurred in high yields (around 70%). The use of phenyl(1-phenylethylidene) (entry 3) and *N*-trimethylsilylbenzaldimine (entries 4) resulted in lower yields (around 50% after 12 h) (Table 1). When species **2** was employed as a catalyst for the imine metathesis reaction in entry 5, the obtained yield was comparable to the same reaction using **3** as a catalyst in entry 2 (around 65% after 12 h).



The conversions for both substrates were similar and the corresponding products were obtained with around the same

Table 1 Catalytic imine metathesis substrate testing using catalysts **3** and **2**

Entry	Imine 5a-5	Cat.	Conv. ^a (%)	Yield (%) 6a-6e	Yield (%) 7a-7e	TON
1		3	75	76	74	19
2		3	65	65	67	16
3		3	54	52	51	13
4		3	48	49	50	12
5		2	66	68	68	17

^a Determined by GC-FID using (4-fluorobenzylidene)-(4-fluorophenyl) as a default substrate after 12 hours.

yield values. Product pairs **6** and **7** are obtained with the same selectivities (50–50%) and no other products were observed.

Additional experiments were performed to test the zirconium system reusability. After 12 h, the catalytic material was isolated by filtration, washed with toluene, dried under high vacuum, and reused in imine metathesis (entry 1). This sequence was performed five times with only a slight loss of catalytic activity being observed (yield of 76% in the first cycle vs. 72% in the fifth cycle) (Fig. S3, ESI†). FT-IR of the catalysts after reaction was conducted which indicates that the catalytically active species are still present and no adsorbed products remain on the surface (Fig. S4, ESI†).

In our investigation of the reactions of $Zr(NEt_2)_4$ with the silica surface to give $[(\equiv Si-O-)Zr(NEt_2)_3]$ (**1**), thermal treatment of **1** generated the imido complex $[(\equiv Si-O-)Zr(=NR)NET_2]$ (**2**). **2** can be converted to $[(\equiv Si-O-)Zr(=NPh)NET_2]$ (**3**) by imine metathesis using $ArC=NPh$. Both **2** and **3** were tested as catalysts for imine metathesis using several imines and exhibited conversion ranging from 49 to 76%. **2** and **3** are the first reported heterogeneous catalysts for imine metathesis.

References

- 1 E. Callens, N. Riache, K. Talbi and J. M. Basset, *Chem. Commun.*, 2015, **51**, 15300–15303.
- 2 N. Riache, E. Callens, J. Espinas, A. Dery, M. K. Samantaray, R. Dey and J. M. Basset, *Catal.: Sci. Technol.*, 2015, **5**, 280–285.
- 3 L. K. Woo, *Chem. Rev.*, 1993, **93**, 1125–1136.
- 4 J. W. Bruno and X. J. Li, *Organometallics*, 2000, **19**, 4672–4674.
- 5 M. Sun, J. Z. Zhang, P. Putaj, V. Caps, F. Lefebvre, J. Pelletier and J. M. Basset, *Chem. Rev.*, 2014, **114**, 981–1019.
- 6 A. Bokka, Y. D. Hua, A. S. Berlin and J. Jeon, *ACS Catal.*, 2015, **5**, 3189–3195.
- 7 C. A. Denard, M. J. Bartlett, Y. J. Wang, L. Lu, J. F. Hartwig and H. M. Zhao, *ACS Catal.*, 2015, **5**, 3817–3822.
- 8 J. I. du Toit, C. G. C. E. van Sittert and H. C. M. Vosloo, *Monatsh. Chem.*, 2015, **146**, 1115–1129.
- 9 J. M. McInnes and P. Mountford, *Chem. Commun.*, 1998, 1669–1670.
- 10 V. C. Gibson, *Adv. Mater.*, 1994, **6**, 37–42.
- 11 W. A. Nugent and B. L. Haymore, *Coord. Chem. Rev.*, 1980, **31**, 123–175.
- 12 A. P. Duncan and R. G. Bergman, *Chem. Rec.*, 2002, **2**, 431–445.
- 13 R. R. Schrock and A. H. Hoveyda, *Angew. Chem., Int. Ed.*, 2003, **42**, 4592–4633.
- 14 P. D. Bolton and P. Mountford, *Adv. Synth. Catal.*, 2005, **347**, 355–366.
- 15 R. L. Zuckerman, S. W. Krska and R. G. Bergman, *J. Am. Chem. Soc.*, 2000, **122**, 751–761.
- 16 K. E. Meyer, P. J. Walsh and R. G. Bergman, *J. Am. Chem. Soc.*, 1994, **116**, 2669–2670.
- 17 K. E. Meyer, P. J. Walsh and R. G. Bergman, *J. Am. Chem. Soc.*, 1995, **117**, 974–985.
- 18 P. Mountford, *Chem. Commun.*, 1997, 2127–2134.
- 19 G. K. Cantrell and T. Y. Meyer, *Organometallics*, 1997, **16**, 5381–5383.
- 20 W. D. Wang and J. H. Espenson, *Organometallics*, 1999, **18**, 5170–5175.
- 21 M. C. Burland, T. W. Pontz and T. Y. Meyer, *Organometallics*, 2002, **21**, 1933–1941.
- 22 J. W. Nelson, L. M. Grundy, Y. F. Dang, Z. X. Wang and X. T. Wang, *Organometallics*, 2014, **33**, 4290–4294.
- 23 J. M. Bates, J. A. M. Lummiss, G. A. Bailey and D. E. Fogg, *ACS Catal.*, 2014, **4**, 2387–2394.
- 24 B. Hamzaoui, M. El Eter, E. Abou-Hamad, Y. Chen, J. D. A. Pelletier and J. M. Basset, *Chem. – Eur. J.*, 2015, **21**, 4294–4299.
- 25 B. Hamzaoui, J. D. A. Pelletier, M. El Eter, Y. Chen, E. Abou-Hamad and J. M. Basset, *Adv. Synth. Catal.*, 2015, **357**, 3148–3154.
- 26 P. Avenier, A. Lessage, M. Taoufik, A. Baudouin, A. De Mallmann, S. Fiddy, M. Vautier, L. Veyre, J. M. Basset, L. Emsley and E. A. Quadrelli, *J. Am. Chem. Soc.*, 2007, **129**, 176–186.
- 27 P. Avenier, X. Solans-Monfort, L. Veyre, F. Renili, J. M. Basset, O. Eisenstein, M. Taoufik and E. A. Quadrelli, *Top. Catal.*, 2009, **52**, 1482–1491.
- 28 F. Blanc, C. Coperet, J. Thivolle-Cazat and J. M. Basset, *Angew. Chem., Int. Ed.*, 2006, **45**, 6201–6203.
- 29 F. Blanc, N. Rendon, R. Berthoud, J. M. Basset, C. Coperet, Z. J. Tonzetich and R. R. Schrock, *Dalton Trans.*, 2008, 3156–3158.
- 30 F. Blanc, J. Thivolle-Cazat, J. M. Basset, C. Coperet, A. S. Hock, Z. J. Tonzetich and R. R. Schrock, *J. Am. Chem. Soc.*, 2007, **129**, 1044–1045.
- 31 D. C. Bradley and I. M. Thomas, *Can. J. Chem.*, 1962, **40**, 1355–1360.
- 32 K. J. Ahmed, M. H. Chisholm, K. Folting and J. C. Huffman, *J. Am. Chem. Soc.*, 1986, **108**, 989–999.
- 33 M. Beaudoin and S. L. Scott, *Organometallics*, 2001, **20**, 237–239.
- 34 M. El Eter, B. Hamzaoui, E. Abou-Hamad, J. D. A. Pelletier and J. M. Basset, *Chem. Commun.*, 2013, **49**, 4616–4618.

